Metallic Glass Nanofibers in Future Hydrogel-based Scaffolds

Ramin Banan Sadeghian-*EMBS Member*, Samad Ahadian-*EMBS Member*, Shin Yaginuma, Javier Ramón-Azcón, Xiaobin Liang, Ken Nakajima, Hitoshi Shiku, Tomokazu Matsue, Koji S. Nakayama, and Ali Khademhosseini-*IEEE Member*

***Abstract*— Electrically conductive reinforced hydrogels offer a wide range of applications as three-dimensional scaffolds in tissue engineering. We report electrical and mechanical characterization of methacrylated gelatin (GelMA) hydrogel, containing palladium-based metallic glass nanofibers (MGNF). Also we show that the fibers are biocompatible and C2C12 myoblasts in particular, planted into the hybrid hydrogel, tend to attach to and elongate along the fibers. The MGNFs in this work were created by gas atomization. Ravel of fibers were embedded in the GelMA prepolymer in two different concentrations (0.5 and 1.0 mg/ml), and then the ensemble was cured under UV light, forming the hybrid hydrogel. The conductivity of the hybrid hydrogel was proportional to the fiber concentration.**

***Index Terms*—Conductive hydrogel scaffolds, Methacrylated gelatin, Metallic glass nanofibers**

I. Introduction

Of late there has been an increasing demand for mechanically strong and conductive hydrogels capable of both hosting and behavioral tailoring of electroactive cells for tissue engineering applications. Reinforcement of such hydrogels is achieved by embedding nanostructures such as gold nanowires, nanotitanate wires, and carbon nanotubes in the hydrogel matrix [1], which is usually accompanied by an increase in the electrical conductivity. While these nanomaterials have proven to be useful in a variety of applications such as monitoring the behavior of engineered tissues and providing mechanical support, there are still open questions on their long-term biocompatibility and endurance.

Metallic glasses are amorphous metals or alloys formed by rapidly cooling the liquid melt causing it to freeze before crystallizing. Because of their porous structure and the absence of grain boundaries, they are often stronger than their crystalline counterparts, are more resistant to corrosion, and have a greater elasticity [2]. Naturally, micro/nano structures of metallic glasses inherit most of the attractive properties of the bulk material, alongside a larger surface-to-volume ratio which is a quantity of interest in the field of biosensing. In addition, fibers made of metallic glass can be stretched to centimeter length scales, far beyond any crystalline nanowire can grow because they have no grain boundaries.

In this work, we demonstrate the application of intertwined nanofibers of a palladium-based metallic glass as a novel biocompatible and reinforcing material incorporated in methacrylated gelatin (GelMA). We show that the electrical conductivity of the metallic glass nanofiber (MGNF)-embedded GelMA can be tuned by varying the concentration of the integrated nanofibers, and the composite can offer a superb elasticity. These properties make the GelMA-MGNF composite particularly handy in hosting skeletal muscle cells where conductivity and elasticity are of utmost importance.

R. Banan Sadeghian is with the WPI Advanced Institute for Materials Research at Tohoku University, Sendai, Japan (phone: +81-022-217-5997; e-mail: ramin@wpi-aimr.tohoku.ac.jp).

II. Experimental Works

We fabricated the MGNFs through gas atomization of $Pd_{42.5}Cu_{30}Ni_{7.5}P_{20}$ (atomic %). Gas atomization, a conventional technique in powder metallurgy, was modified for the formation of nanofibers [3]. Briefly, the alloy was melted through inductive heating in a quartz crucible, forced through the crucible nozzles, and then blown by high pressure gas jets forming the nanofibers at the end. The viscosity of the molten alloy and the gas jet pressure determine the size and shape of the nanofibers. Here the gas pressure and the crucible temperature were 10 MPa and 520 °C respectively. Fig. 1a and 1b show a snapshot and an SEM micrograph of the entangled MGNFs. The smoothness of the fiber surface is discernible in the magnified view in the inset of Fig. 1b. The mean diameter of the fibers is 700 nm.

GelMA prepolymer was synthesized as described earlier [4]. Impregnation-ready GelMA hydrogel was prepared by dissolving a mixture of the prepolymer with 1% (w/v) photoinitiator (Irgacure 2959) in Dulbecco's phosphate-buffered saline (DPBS). The solution was then warmed up to 40 °C before using in the experiments.

Pristine solution of GelMA and hybrid GelMA-MGNF hydrogels with MGNF concentrations of 0.5 and 1.0 mg/ml were prepared for electrical characterization. After being exposed to UV light for 60 seconds to induce polymer cross-linking, the samples were confined between two indium tin oxide (ITO) coated glass slides. The effective electrode area and the interelectrode spacing of the capacitor-like devices were 1.2 cm^2 and 50 μm respectively. DC current-voltage (I-V) characteristics were measured by performing a step-wise voltage sweep from -6.0 to 6.0 V (ΔV = 0.1 V, Δt = 0.1 s) using a source-measure unit (SMU) of a Keithley 4200 semiconductor parameter analyzer. Frequency domain measurements were taken using an LCR meter (HP 4263B) at frequencies of 100 Hz, 1 kHz, 10 kHz, and 100 kHz, and a test signal level of 1 V_{rms}.

We cultured 3T3 fibroblasts and C2C12 myoblasts until reaching 70–80% confluency. The cells were trypsinized and then encapsulated in the pristine and hybrid hydrogels, with a density of 10^7 cells per milliliter, by mixing in 5% (w/v) prepolymer. After curing by UV light, cell-laden hydrogels were stored in additional culture medium until

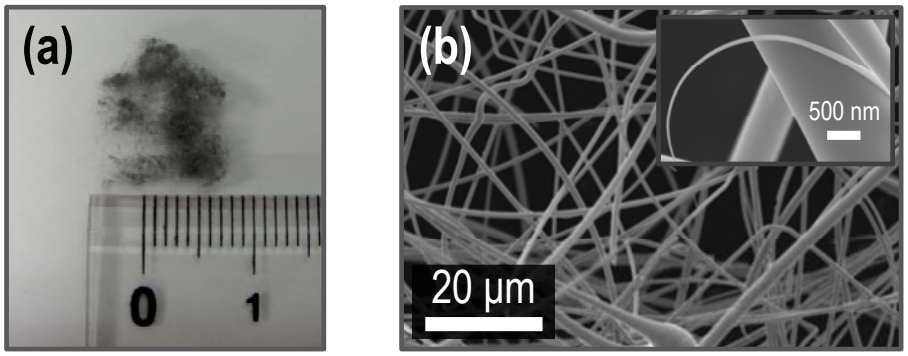

Figure 1. a) A snapshot and b) an SEM micrograph of a cluster of MGNFs. The magnified view in the inset shows the smoothness of the fiber surface.

used for cell viability and growth assessments through immunostaining and polymerase chain reaction (PCR) analysis. We utilized calcein-AM and ethidium homodimer live/dead probes (Invitrogen, USA) for quantification of the viability of fibroblasts in pristine GelMA and in the GelMA-MGNF hybrid. The former probe is converted to green in alive cells, while the latter enters the damaged cell membranes and stains them red. Cellular alignment and elongation are desirable in tissue engineering wherever anisotropic properties are sought. Cellular aspect ratio, defined as the ratio of major to minor axes, determines the quantity of elongation. We employed DAPI and phalloidin immunostaining to reveal the cell nuclei and F-actin, respectively. The percentage of live fibroblast and the aspect ratios of C2C12 myoblasts were quantified using the National Institute of Health ImageJ software.

III. Results and Discussion

Fig. 2 shows the *I-V* characteristics of the devices comprised of pristine and hybrid (1.0 mg/ml of MGNF) hydrogels. To gain insight into the response of GelMA as an electrolyte enclosed between pair of electrodes, a two-way voltage sweep was performed. The *I-V* dependence of the pristine GelMA device was found to be nonlinear. As shown in the inset, the anodic and cathodic peaks associated with faradaic currents are discernible at low voltages.

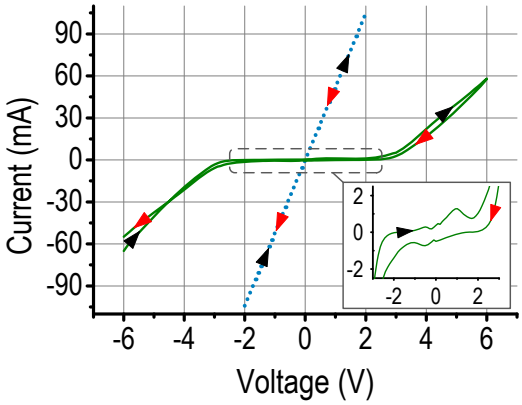

Figure 2. *I-V* curves corresponding to the pristine (green solid line) and the hybrid hydrogel with 1.0 mg/ml of MGNFs (blue dotted line). Black and red (dark and bright) arrows indicate the direction of the voltage sweep. Inset: Magnification of the central part of the voltammogram showing the cathodic and anodic peaks of pristine GelMA.

Notice that the *I-V* curves are not cyclic voltammograms normally recorded from a three-electrode electrochemical cell. As a result, the redox potential/current peak pairs observed here cannot be precisely quantified and associated to electrode reactions. As the applied voltage increased, for $|V| \gtrsim 3$ V, the hydrogel containing medium (DPBS) suffered from electrolysis and GelMA became conductive. Obviously, the resistance of pristine GelMA prior to electrolysis was very high (in the gigaohm range or higher), and hence could not be quantified with our Keithley SMU.

The hybrid hydrogel in contrast, displayed an ohmic behavior where the resistances, extracted from the slope of the plots, were almost inversely proportional to the amount of embedded nanofibers. Table I shows the values of measured resistances versus the concentration of embedded MGNFs in 5% GelMA. The small discrepancy in the above trend can be attributed to the uncertainly in the amount of MGNFs and the inhomogeneity of spreading the ravel of fibers in GelMA. These results demonstrate the feasibility of tuning the conductivity of GelMA by the concentration of embedded conductive nanofibers.

To conduct frequency domain measurements, three capacitor-like constructs were fabricated similar to those made for DC characterization; one with pristine GelMA, and two other with GelMA-MGNF hybrid hydrogels containing 0.5 and 1.0 mg/ml of MGNFs. The impedance Bode plots of the devices are presented in Fig. 3. The measured frequency response was applied to the Randles equivalent circuit [5] (Fig. 4a) to obtain the variation of parallel resistance, R_p, and capacitance, C_p, with frequency (Fig. 4b and 4c). The series resistance, R_s, was less than an ohm and therefore negligible. The mobilities of ions in the hydrogel are limited, as a result not all of the electrode area will be charged by ions at high frequencies causing the capacitance to roll-off in a similar fashion to electrolytic capacitors. At low frequencies, R_p declined steadily with increasing frequency and crossed over to an invariant value.

Table I.
Resistances of the Hybrid Hydrogel Device versus the Concentration of Nanofibers

MGNF concentration (mg/ml)	*Resistance (Ω)*
0.5	33.5
1.0	19.2

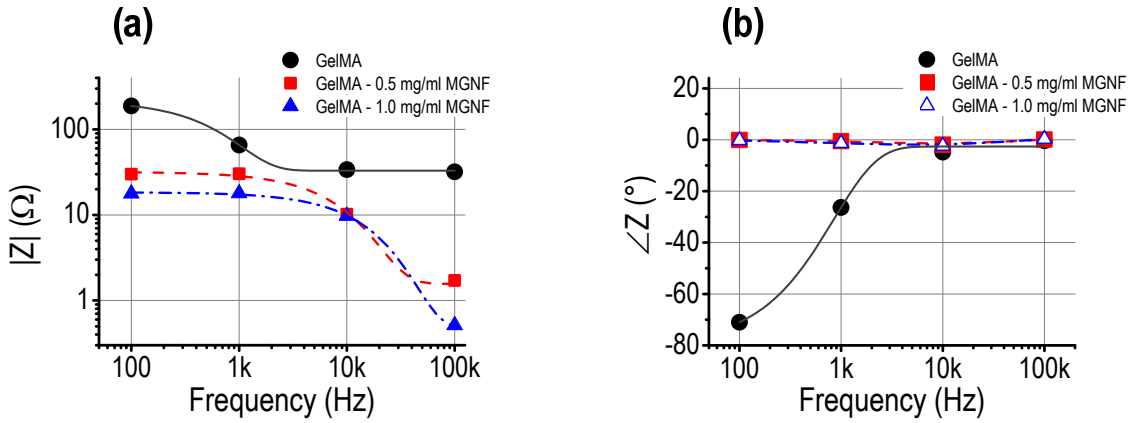

Figure 3. (a) Magnitude, and (b) phase angle Bode plots of the impedance spectra obtained from devices containing pristine GelMA and GelMA-MGNF hybrid hydrogel with two different nanofiber concentrations.

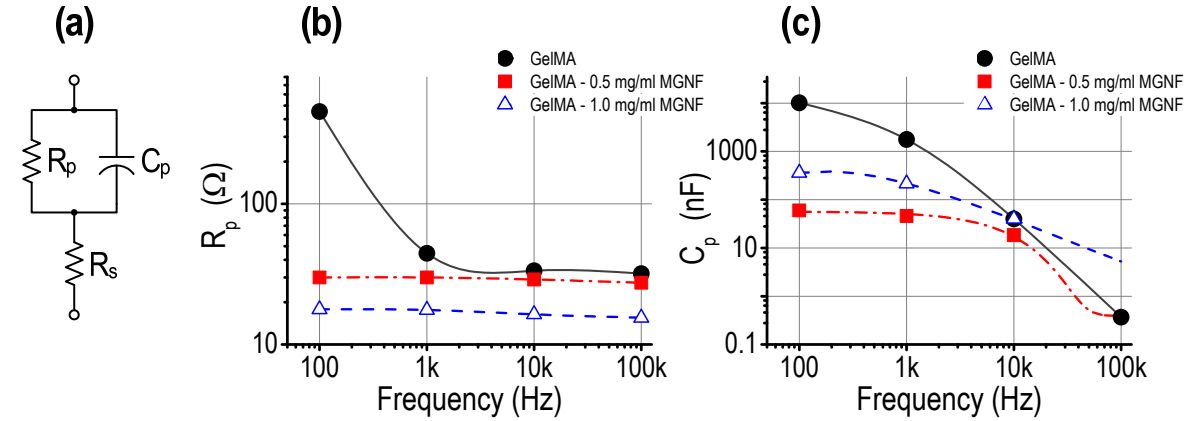

Figure 4. (a) Equivalent circuit for modeling the frequency response of GelMA and GelMA-MGNF hybrid hydrogel. (b) Parallel resistance and (c) capacitance of the devices extracted from the impedance data.

Micromechanical maps of the pristine and hybrid hydrogels were recorded by Atomic Force Microscopy (AFM) and the data were used to compute and compare the mechanical properties of both hydrogels. Table II shows the Young's moduli of three samples extracted from 200 representative points of the corresponding modulus map. As expected, the Young's modulus of the hybrid hydrogel increases with nanofiber concentration.

Earlier studies have confirmed both the biocompatibility and the biodegradability of metallic glass materials in cells as well as in tissues [6, 7]. To study the biocompatibility of our metallic glass fibers, cell-laden GelMA-MGNF hybrid hydrogels were prepared, cured, and examined. After two days of culture, there was no significant difference between the viability of fibroblasts in pristine GelMA and those embedded within the GelMA-MGNF hybrid containing 1.0 mg/ml of nanofibers. Fig. 5a shows the viability data collected over two consecutive days of culture.

We also assessed the morphology, adhesion, and growth of C2C12 myoblasts on the first and second days of culture by immunofluorescence observations of the cytoskeletal structures, followed by gene expression analysis. Myoblasts cultured in the hybrid hydrogel (containing 1.0 mg/ml of MGNFs) demonstrated a considerable increase in their aspect ratios. Fig. 5b compares the aspect ratios of the muscle cells grown in these two media, on day 1 and day 2. Fig. 6 shows four C2C12 cells attached to and stretched along a single MGNF in GelMA. As shown previously, C2C12 myoblasts can be affected by the morphology and conductivity of their supporting scaffolds and exhibit enhanced adhesion and spreading on conductive surfaces, e.g. on carbon nanotubes [8]. These results suggest that muscle cells cultured in the GelMA-MGNF hybrid develop to be longer than those grown in pristine GelMA and can make stronger functional tissues.

Expression levels of four genes pertinent to adhesion, growth, and focal adhesion components of C2C12 myoblasts cultured in hybrid and pristine hydrogels were measured separately in two consecutive days of culture. The gene expression levels (GEL) of both cases were first normalized to the corresponding values obtained from a house gene, GAPDH, and then the ratios were calculated in percentage using Equation (1) and presented in Table III.

TABLE II.
YOUNG MODULI OF PRISTINE AND HYBRID GELMA VERSUS THE CONCENTRATION OF NANOFIBERS

MGNF concentration (mg/ml)	*Young's modulus (Pa)*
0 (pristine)	472 ± 121
1.0	1029 ± 638
2.0	3985 ± 1351

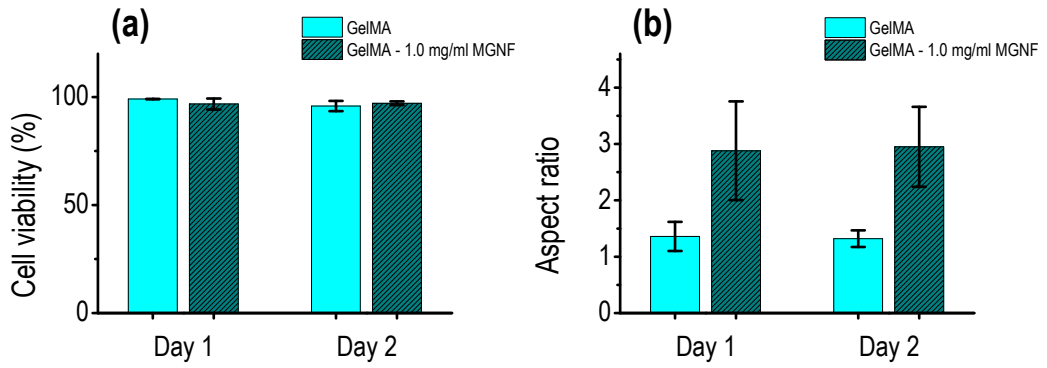

Figure 5. a) Percentage of alive fibroblasts, and b) aspect ratios of C2C12 myoblasts in pristine GelMA and GelMA-MGNF hybrid hydrogels.

$$\text{GEL ratio} = \frac{\text{Normalized GEL in pristine GelMA}}{\text{Normalized GEL in the hybrid hydrogel}} \times 100\% \quad (1)$$

A significantly higher expression levels of the underlying genes were observed in the muscle cells cultured in the GelMA-MGNF hybrid than those grown in pristine GelMA. For example, a 'Day 1' focal adhesion kinase (FAK) value of 0.02% means that FAK has been amplified 5000 times in the hybrid hydrogel, and 0.3% for integrin implies that this gene was expressed about 300 times more at 'Day 2'. These results indicate that the GelMA-MGNF hybrid is more favorable that pristine GelMA in regulating the adhesion and spreading behaviors of muscle cells, most likely because of the combined morphological and electrical cues of the MGNFs.

The hybrid hydrogel introduced in this work offers implications as a host for electroactive cells because of its tunable conductivity and enhanced mechanical strength. Potential applications include, but are not limited to scaffolds for functional muscle tissues and biosensors.

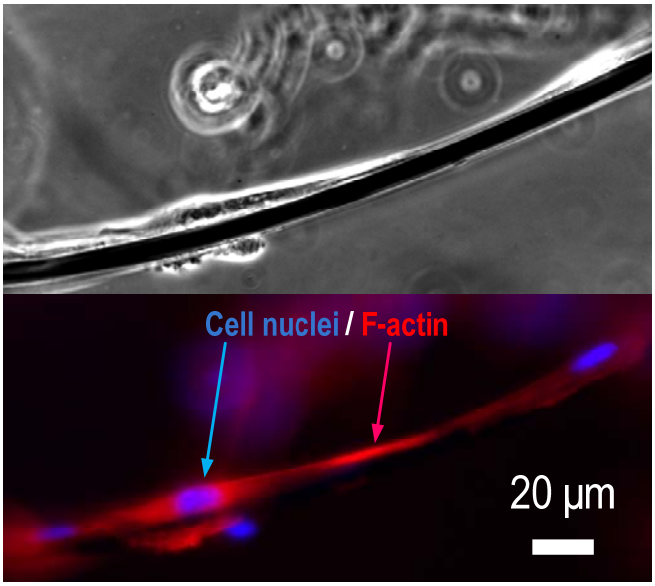

Figure 6. Optical (top) and fluorescent (bottom) images of C2C12 myoblasts attached on a single MGNF in GelMA.

TABLE III.
RATIOS OF NORMALIZED GELS OF C2C12 CELLS CULTURED IN PRISTINE GELMA TO THOSE CULTURED IN THE HYBRID HYDROGEL[a]

Gene	Expression level ratios × 100%	
	Day 1	*Day 2*
Integrin	39.2	0.30
FAK	0.02	9.60
Collagen type I	0.11	4.40
Vinculin	0.25	8.57

a. containing 1.0 mg/ml of MGNFs

IV. CONCLUSIONS

GelMA itself is a nonconductive gel with many attractive tissue-like properties. Here we showed that it can be made conductive and mechanically strengthened by addition of Pd-based MGNFs. The resulting hybrid hydrogel proved to be biocompatible and in addition, favorable in regulating the adhesion and elongation of skeletal muscle cells.

REFERENCES

[1] T. Dvir, B. P. Timko, D. S. Kohane, and R. Langer, "Nanotechnological strategies for engineering complex tissues," *Nat Nanotechnol*, vol. 6, pp. 13–22, 2011.

[2] M. Telford, "The case for bulk metallic glass," *Materials Today*, vol. 7, pp. 36–43, 2004.

[3] K. S. Nakayama, Y. Yokoyama, T. Wada, N. Chen, and A. Inoue, "Formation of Metallic Glass Nanowires by Gas Atomization," *Nano Letters*, vol. 12, pp. 2404–2407, 2012.

[4] J. Ramon-Azcon, S. Ahadian, R. Obregon, G. Camci-Unal, S. Ostrovidov, V. Hosseini, et al., "Gelatin methacrylate as a promising hydrogel for 3D microscale organization and proliferation of dielectrophoretically patterned cells," *Lab on a Chip*, vol. 12, pp. 2959–2969, 2012.

[5] N. Tandon, A. Marsano, R. Maidhof, K. Numata, C. Montouri-Sorrentino, C. Cannizzaro, et al., "Surface-patterned electrode bioreactor for electrical stimulation," *Lab on a Chip*, vol. 10, pp. 692–700, 2010.

[6] L. Huang, Z. Cao, H. M. Meyer, P. K. Liaw, E. Garlea, J. R. Dunlap, et al., "Responses of bone-forming cells on pre-immersed Zr-based bulk metallic glasses: Effects of composition and roughness," *Acta Biomaterialia*, vol. 7, pp. 395–405, 2011.

[7] B. Zberg, P. J. Uggowitzer, and J. F. Loffler, "MgZnCa glasses without clinically observable hydrogen evolution for biodegradable implants," *Nat Mater*, vol. 8, pp. 887–891, 2009.

[8] T. Fujie, S. Ahadian, H. Liu, H. Chang, S. Ostrovidov, H. Wu, et al., "Engineered Nanomembranes for Directing Cellular Organization Toward Flexible Biodevices," *Nano Letters*, vol. 13, pp. 3185–3192, 2013.